

MECHANICAL DESIGN OF PULSE-BY-PULSE X-RAY BEAM POSITION MONITOR USING DIAMOND HEAT SINK*

Hideki Aoyagi[†], Sunao Takahashi,
Japan Synchrotron Radiation Research Institute (JASRI), Hyogo, Japan

Abstract

It is indispensable to diagnose dynamics of synchrotron radiation beam for stable supply of the beam in synchrotron radiation facilities. We are developing a pulse-by-pulse X-ray beam position monitor using diamond heat sinks for an undulator beamline. We have designed the monitor aiming at improving heat-resistance property without degradation of high frequency property, and manufactured a prototype to evaluate a feasibility of the design. Thermal finite element analysis was carried out to design an effective structure of a detector head and a holder. Time-domain reflectometry was utilized to evaluate high frequency property of the prototype.

INTRODUCTION

A conventional X-ray beam position monitor (XBPM) is photoemission type, and blade-shaped tungsten is used as detector heads to secure heat resistance. Stabilization of pulse-by-pulse electron beam position has been realized at a high level in the SPring-8 storage ring [1,2]. The conventional XBPM, however, cannot measure pulse-by-pulse beam position, because the time constant of the detector head is long due to the stray capacitance and the impedance is not matched to 50 Ω of cables. To overcome this problem, a pulse-by-pulse XBPM equipped with microstripline structure (stripline-XBPM), which also works as a photocathode, had been developed for the SPring-8 bending magnet (BM) beamlines [3,4]. This monitor has potential to function as (1) a pulse intensity monitor, (2) a pulse-by-pulse XBPM, and (3) a pulse timing monitor [5]. For the undulator beamlines, further improvement of heat-resistance is required. Therefore, we are developing a pulse-by-pulse XBPM for undulator beamlines by introducing heat resistance structure that employed a diamond heat sink.

STRUCTURE OF PROTOTYPE

We started a design work for realization of the pulse-by-pulse XBPM from the following points of view. We decided to suppress an increase in time constant ($t = RC$) by lowering the stray capacitance as much as possible with securing an effective area of a photocathode, while accepting impedance mismatch around the photocathode [6]. As shown in Fig. 1, the photocathode is mounted on a diamond heat sink as a detector head. We adopted heat-resistant structure to reduce an effective irradiation cross section by aligning four detector heads parallel to a beam axis. A heat sink holder is attached to a cooling base welded to a DN40CF (ICF70) flange. A signal transfer line having microstripline structure is mounted on another ICF70 flange

* This work was partly supported by Japan Society for the Promotion of Science through a Grant-in-Aid for Scientific Research (c), No. 20416374.

[†] aoyagi@spring8.or.jp

[7]. By separating signal transfer line from cooling mechanism, although high frequency property is degraded compared with the stripline-XBPM mentioned above, the heat-resistant property is expected to be improved. Figure 2 shows a prototype with a 6-way cross chamber. A couple of ICF70 flanges equipped with the detector heads (the signal transfer lines) are mounted on the top/bottom (left/right) ports. Two beam ports are faced using DN63CF (ICF114) flanges with a face-to-face dimension of 120 mm.

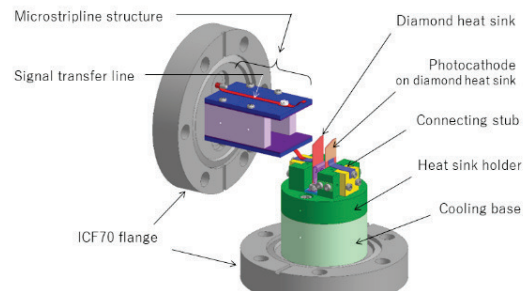


Figure 1: 3D image of the cooling structure (bottom) and the microstripline structure (left).

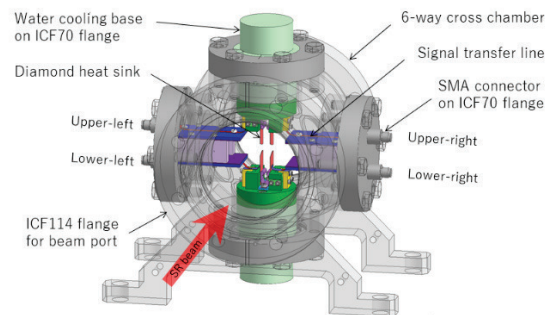


Figure 2: 3D image of the prototype.

THERMAL FINITE ELEMENT ANALYSIS

The thermal finite element analysis (FEA, ANSYS® Release 17.0) was carried out on the diamond heat sink (20 mm \times 8 mm \times 0.3 mm), the heat sink holder and the cooling base. A quarter model was used for the analysis, and the heat sink holder and the cooling base are treated as an integrated object for simplification. Figure 3 shows an analysis result of the typical case in the normal operation of the SPring-8 standard undulator beamlines. The thermal conductance (TC) of diamond and copper are set to 1,500 and 400 W/(m \cdot K), respectively. Thermal contact conductance (TCC) between the diamond heat sink and the heat sink holder made of copper is assumed to be 10,000W/(m 2 \cdot K) in this calculation. The total power of 10W is input with uniform heat flux on the tip (1 mm \times 8 mm \times 0.3 mm) of the heat sink. This input power is equivalent to the maximum value assumed in the normal operation. The homoiothermal condition (30°C) is put to the bottom of the cooling

Content from this work may be used under the terms of the CC BY 3.0 licence © 2016. Any distribution of this work must maintain attribution to the author(s), title of the work, publisher, and DOI.

base. If the tolerance of the temperature rise is set as $\Delta t = 100$ K for a realistic value, the analysis result of this representative model is within the tolerance.

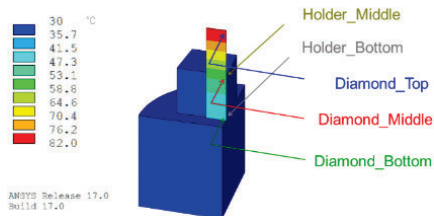


Figure 3: Quarter model for the FEA and the results. Arrows indicate locations of measuring points.

The temperature at each point on condition that the TC of the diamond is $1,500 \text{ W}/(\text{m}\cdot\text{K})$ is plotted as a function of the TCC between the diamond sink and the copper, as shown in Fig. 4. This result suggests that the TCC is not so effective for heat-resistance property if the TCC exceeds $10,000 \text{ W}/(\text{m}^2\cdot\text{K})$, and that, on the other hand, the temperature rise exceeds the tolerance of 100 K if the TCC below $2,000 \text{ W}/(\text{m}^2\cdot\text{K})$.

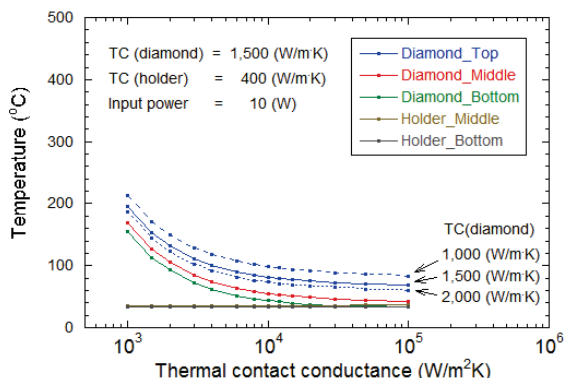


Figure 4: Thermal contact conductance (TCC) dependence of temperature.

Figure 5 shows the temperature variations by the difference in the TC of blade material used for the heat sink on condition that the TCC is $10,000 \text{ W}/(\text{m}^2\cdot\text{K})$. If the TC of diamond is higher than $1,500 \text{ W}/(\text{m}\cdot\text{K})$, the temperature rise is suppressed reasonably, and it is not required to know the exact number of the TC of diamond. If copper or tungsten plates are used for the heat sink, the temperature rise would exceed the tolerance level.

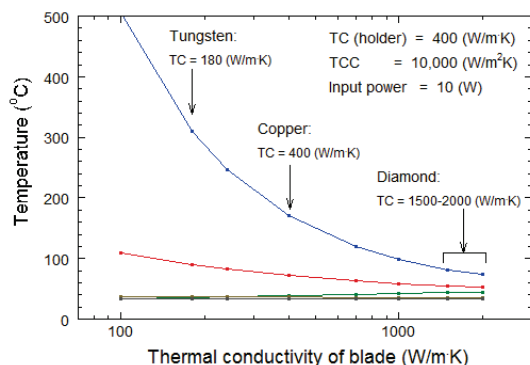


Figure 5: Thermal conductivity (TC) dependence of temperature.

The maximum input power reaches around 25 W during commissioning/tuning of beamlines. Figure 6 shows the expected temperature of each point as a function of the input power, when the TCC is assumed to be $10,000 \text{ W}/(\text{m}^2\cdot\text{K})$. The calculation shows that the current design is practicable.

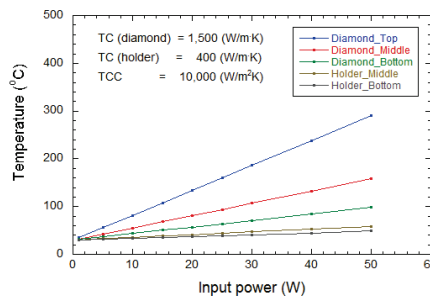


Figure 6: Input power dependence of temperature.

TIME-DOMAIN REFLECTOMETRY

A time-domain reflectometry (TDR) by using a single input pulse was utilized to evaluate high frequency property of this monitor. Although either a rising or a falling edge of rectangular wave is usually used for TDR, we used the isolated single pulse with unipolar (140 ps FWHM) for an input signal because of easiness of the interpretation.

The actual role of this monitor is to propagate an impulse from a tip of the detector head to the measuring instrument through the signal transfer line. Therefore, it is possible to predict a time structure of an actual output signal by observing the isolated single pulse that is input directly from the detector head through a probe, namely, a time-domain transmissometry (TDT). We discuss about the results using TDR here, because it has been already confirmed that the results from TDR resembles those from TDT [8].

As shown in Fig. 7, the input pulse from a pulse generator branches into an oscilloscope (4 GHz , 20 GS/s) and measured objects with a divider. The reflected signal makes a round trip along the cable (1 m), and about 10 ns later it is observed with the oscilloscope.

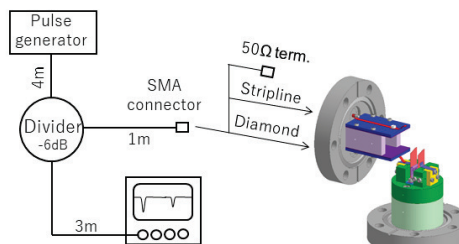


Figure 7: Experimental setup for the time-domain reflectometry.

As shown in Fig. 8, the peaks at $t = 0 \text{ ns}$ is the input pulse observed directly. The pulse shapes observed at $t = 9 \sim 10 \text{ ns}$ are the reflected pulse as follows: (1) SMA connector with 50Ω termination (light green), (2) SMA connector with open end (green), (3) with microstripline structure (blue), (4) with microstripline structure and a connecting stub (purple), (5) with microstripline structure, a connecting stub and a diamond heat sink (red). There is delay of

0.7 ns, which corresponds to the length of microstripline structure, in the reflected signal with microstripline structure (blue), compared with the reflected signal from the SMA with open end (green). The time structure is almost maintained. The double peak was observed in the reflected signal from the diamond heat sink (red), which has an electrode as the photocathode. This is the result of impedance mismatching of the section between the microstripline structure and the electrode on the diamond heat sink.

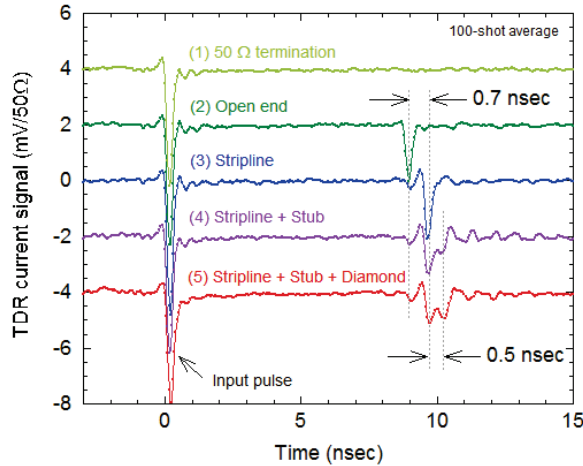


Figure 8: Experimental results of Time-domain reflectometry.

To consider the relation between the results obtained by TDR and the waveform generated actually from a monitor, three kinds of diamond device, as shown in Fig. 9, were compared: (a) the diamond heat sink with an electrode introduced this time, (b) a dummy diamond plate prepared for a preliminary study, and (c) a diamond semiconductor detector developed as an electron beam halo monitor [9].

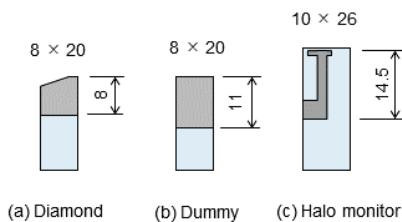


Figure 9: Structure of heat sinks and a diamond detector. Shaded areas are electrodes. The thickness is 0.3mm.

As shown in Fig. 10, (5), (6) and (7) are reflected pulses in TDR from the diamond devices of (a), (b) and (c), respectively. The waveform generated actually from a detector of the halo monitor actually (blue) is also indicated by shifting a time axis. The pulse length of the actual pulse (blue) is 0.4 ns FWHM, while the width of the double peak (black) seen in TDR of (c) is 0.5 ns. The width of the double peak of the diamond heat sink (5) is narrower than that of the dummy plate (6), because the diamond heat sink is designed to have a smaller electrode. These results suggest that this monitor generates the unipolar pulse signal with the pulse length of sub-nanosecond.

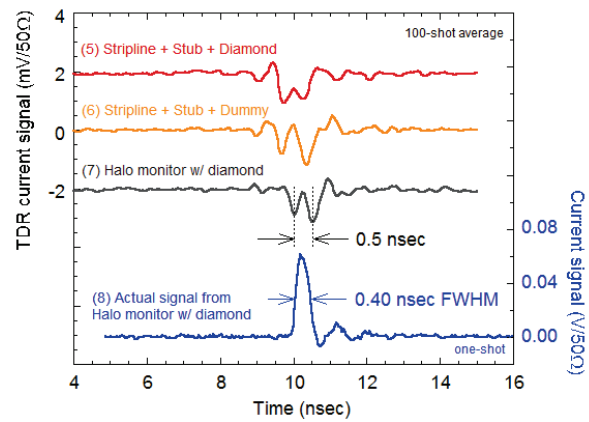


Figure 10: Comparison of the results of time-domain reflectometry with an actual pulse shape of the halo monitor.

SUMMARY

We have designed the pulse-by-pulse X-ray beam position monitor using the diamond heat sink, and manufactured the prototype to evaluate the thermal and high frequency properties. The results of thermal finite element analyses suggest that the diamond heat sink mounted on the holder described here is practicable from the heat-resistant point of view, if the TCC between diamond and copper is assumed to be $10,000 \text{ W}/(\text{m}^2 \cdot \text{K})$. The evaluation tests of the prototype on high frequency property using TDR suggest that the single isolation pulse of the sub-nanosecond can be provided.

It's necessary to estimate experimentally the thermal contact conductance between the diamond heat sink and the heat sink holder made of copper in the next step. Furthermore, we are planning to manufacture a real component, to install it into the beam line, and to carry out overall performance tests.

ACKNOWLEDGEMENT

The authors would like to thank T. Nakamura, K. Kobayashi, S. Kimura and H. Osawa of Japan Synchrotron Radiation Research Institute (JASRI) for the useful advice regarding high frequency analysis. The design and fabrication of the prototype of the pulse-by-pulse XBPM has been achieved by getting cooperation of Vacuum and Optical Instruments (Shinku-Kogaku, Inc, Tokyo, Japan).

REFERENCES

- [1] T. Nakamura et al., Proc. EPAC 2004, 2646.
- [2] T. Nakamura, K. Kobayashi, Proc. ICALEPCS 2005, PO2.022-2.
- [3] H. Aoyagi et al., Proc. PASJ2006, TO25, 159-162.
- [4] H. Aoyagi et al., AIP Conf. Proc. 879, 1018 (2007).
- [5] H. Aoyagi et al., Proc. DIPAC2011, MOPD91, 260-262.
- [6] H. Aoyagi et al., Proc. PASJ2015, THP085, 1224-1226.
- [7] H. Aoyagi et al., Phys. Rev. ST Accel. Beams 16, 032802.
- [8] H. Aoyagi et al., Proc. PASJ2016, TUP086.
- [9] H. Aoyagi et al., Phys. Rev. ST Accel. Beams 15, 022801.